Fabrication of ultrafiltration membranes by poly (aryl ether nitrile) with poly (ethylene glycol) as additives

Qi Wang, Fengna Dai, Shangying Zhang, Chunhai Chen and Youhai Yu

ABSTRACT

A new kind of flat sheet ultrafiltration membrane was prepared by a promising membrane material, poly (aryl ether nitrile) (PEN), via non-solvent induced phase separation. The effect of solvents, N-methyl-2-pyrrolidone (NMP) and dimethyl acetamide (DMAc), as well as additive of poly (ethylene glycol) (PEG) with different molecular weights on the structure and permeation performance of synthesized membranes were investigated. Comparing with NMP, DMAc is more suitable for the casting solution preparation due to better solubility. A gradually changing pore from sponge-like to finger-like can be observed when PEG was added with DMAc as solvent, while a finger-like pore structure always appears in the NMP system with or without PEG. In both systems, the formation of macrovoids is effectively promoted by the addition of PEG, and higher porosity membranes can be obtained by PEG with higher molecular weight. With the increase of PEG molecular weight from 400 to 10,000 Da, the permeate flux increases from 74.5 to 114.3 $L \cdot m^{-2} \cdot h^{-1}$ and from 102.0 to 130.8 $L \cdot m^{-2} \cdot h^{-1}$ under a 100 kPa pressure-driven when NMP and DMAc were used as solvents, respectively. The membranes prepared by DMAc exhibit outstanding rejection of BSA with rejections all above 96.5%.

Key words | non-solvent induced phase separation, poly (aryl ether nitrile) membranes, poly (ethylene glycol), ultrafiltration

Qi Wang
Fengna Dai
Shangying Zhang
Chunhai Chen
Youhai Yu (corresponding author)
Center for Advanced Low-Dimension Materials, State Key Laboratory for Modification of Chemical Fibers and Polymer Materials, College of Material Science and Engineering,
Donghua University,
Shanghai 201620,
China
E-mail: *yuyouhai@dhu.edu.cn*

HIGHLIGHTS

- Poly (aryl ether nitrile) was used to prepare a porous polymeric membrane via non-solvent induced phase separation.
- The choice of solvent and PEG molecular weight have a significant effect on the structure and performance of the PEN membrane.
- Under 0.1 MPa pressure, the final PEN membrane reach a permeate flux of 130.8 $L \cdot m^{-2} \cdot h^{-1}$, while taking into account the high BSA retention performance of 96.5%.

INTRODUCTION

Membrane technology has been considered as an attractive separation technique due to the advantage of efficient operation and low energy consumption (Weatherley 1994). Ultrafiltration membranes with a pore size between 2 and 100 nm have a broad application in pharmaceutical, chemical, food industry, biological macromolecules processing, wastewater treatment and so on (Yi *et al.* 2012). According to the composition, the ultrafiltration membranes can be classified into two major groups of polymeric membranes and ceramic membranes. At present, the dominating membrane material for ultrafiltration is polymers, which have the properties of good film forming capability, mechanical strength and relatively low fabrication cost. Polymer materials, such as polysulfone, poly (ether ether ketone), poly (ether sulfone), poly (vinylidene fluoride), polyimide and cellulose acetate have been widely studied and are well-accepted polymers for membrane fabrication. However, membrane fouling, caused by the hydrophobic properties of

doi: 10.2166/wst.2020.529

these materials, is considered as the obstacle hindering wider spread of membrane technology applications (Koehler *et al.* 1997; Idris *et al.* 2007). Many investigators have demonstrated that hydrophilic modification of a hydrophobic membrane is an efficient strategy to reduce membrane fouling (Braeken *et al.* 2006; Park *et al.* 2006).

PEN, a semi-crystalline polymer belonging to a class of poly (aryl ethers), possesses attractive properties such as excellent resistance to heat, solvents and radiation as well as good mechanical properties: 'The inherent viscosities of PEN was in the range of 0.46 to 1.70 dL/g, the glass transition temperature of PEN was in the range of 148 to 313 °C, and the tensile strength can reach 158 MPa' (Matsuo *et al.* 1993; Lignier *et al.* 2011). PEN has a poly (m-phenylene ether) structure with pendant nitrile groups. Considering that -CN group can be hydrolyzed to -COOH group under basic conditions to improve the hydrophilic property of the body material (Gutmann & Obermayer 2010; Pu & Lan 2013), we believe that PEN is a promising antifouling membrane material. Until now, few studies have reported the application of PEN as a separation membrane material in water treatment. The study of Zhang *et al.* using hydrophilic PEG800 as a pore-forming agent to improve the permeability of membranes showed that as the content of PEG800 increased, the permeability increased significantly, while the corresponding selectivity decreased (Zhang *et al.* 2019). Zhang *et al.* reported that PEN nanofibrous substrate was prepared by electrospinning, and polydopamine-modified hexagonal boron nitride (h-BN-PDA) was self-assembled on the PEN nanofibrous mat to prepare the nanofibrous composite membrane. Due to the synergistic effect of the h-BN-PDA surface layer and PEN support layer, the prepared composite membrane exhibits superhydrophilic/underwater superoleophobic property (Zhang *et al.* 2020). In this work, we focus on the preparation and separation performance study of PEN-based membrane.

Since the discover of phase inversion by Loeb and Sourirajan in 1963, it has been the most extensively used process for preparing polymeric membranes. In this process, the exchanging of solvent with non-solvent in an immersion bath induces the phase separation of homogeneous dope solution into a polymer-rich phase and a polymer-poor one to form a symmetric or asymmetric structure as the continuation of phase separation and the solidification of the polymer-rich phase. It is well accepted that both the thermodynamic parameters such as the interaction between polymer, solvent and nonsolvent, as well as the kinetic parameters such as exchange rate between solvent and nonsolvent, influence performance of the final membranes (Machado & Habert 1999; Han & Nam 2002). Considering water is usually used as a non-solvent coagulation bath, the solvent selection is very important to a given polymer for the membrane fabrication (Madaeni & Rahimpour 2010; Sun *et al.* 2010). Apart from polymer, solvent and non-solvent, incorporation of additives in the casting solution also plays a crucial role to obtain polymeric membrane with desired structure and property. The additive, which can be inorganic or organic, affects the final character of membranes through changing either phase separation kinetics or thermodynamic or solvent capacity (Miteva *et al.* 2017; Oskoui *et al.* 2019).

PEG, a nontoxic hydrophilic polymer, has been widely used as an additive to enhance the hydrophilic properties as well as improve the pore interconnectivity of the resulting membrane (Chakrabarty *et al.* 2008; Gao *et al.* 2018; Sun & Yang 2018). The membrane characteristics, such as morphology, pure water flux and selective permeability, were influenced by the concentration and molecular weight of PEG.

In this work, two solvents, NMP and DMAc, were chosen to prepare PEN flat sheet ultrafiltration membranes by the NIPS method with PEG as additives. The effect of solvent and PEG molecular weight on the structure and permeation properties of membranes were studied in detail.

EXPERIMENTAL

Materials

PEN with $[\eta]$ of 1.15 dL/g was synthesized in the laboratory according to Tang's description (Tang *et al.* 2011). Reagent grade PEG with an average molecular weight of 400 Da, 6,000 Da and 10,000 Da was supplied by Macklin Biochemical Technology Ltd, Shanghai. The chemical structures of PEN and PEG are shown in Figure 1. Reagent grade NMP and DMAc supplied by Macklin were used as received. Deionized water purified by Millipore system (Millipore, France) was used as the coagulation bath. Bovine serum albumin (BSA) with molecular weight of 68,000 Da was obtained from Energy Chemical Ltd, Shanghai.

Membrane preparation

PEN membranes were prepared by NIPS. Briefly, PEN was dissolved in NMP or DMAc, at room temperature with relative humidity of ≤70%. Then PEG with different molecular weights (400 Da, 6,000 Da and 10,000 Da) was added. The composition of each casting solution is shown in Table 1, the concentration for PEN and PEG was kept as 18wt% and 10wt% to ensure the formation of defect-free film.

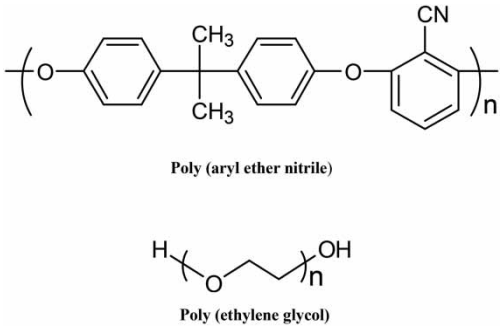

Figure 1 | Molecular structure of poly (aryl ether nitrile) and poly (ethylene glycol).

Different compositions of membrane were designated as PEN/NMP, PEN/NMP/PEG*X*, PEN/DMAc and PEN/DMAc/PEG*X*, where *X* represents the molecular weight of PEG. After continuous stirring and heating at 60 °C, a homogeneous solution was prepared. Then, the casting solution was spread uniformly on a clean glass (12 cm × 12 cm) by a casting knife with a clearance of approximately 100 μm. The primary membranes were exposed for about 25 s to ambient before immersion into the deionized water at room temperature. The color of membraned changed from transparent to white immediately on immersing into the coagulation bath. After sufficient solvent and non-solvent exchanging time, the fully cured film would automatically fall from the glass plate. Then excess solvent and additive were removed by multiple water changes. Finally, the membranes were cut into rectangles with a size of 8.50 cm × 3.50 cm and saved in water before testing.

Characterization methods

The apparent viscosity of each casting solution was measured using a rotational Viscometer (HAAKE Viscotester E) with a unified selection of No. 4 rotor at 30 °C.

Table 1 | Composition of the casting solutions

Membranes	PEG (wt%)			Solvent (wt%)		Solution viscosity (cP)
	400	6,000	10,000	NMP	DMAc	
PEN/NMP				82		54,536
PEN/NMP/PEG*400*	10			72		49,960
PEN/NMP/PEG*6000*		10		72		64,268
PEN/NMP/PEG*10000*			10	72		66,874
PEN/DMAc					82	28,655
PEN/DMAc/PEG*400*	10				72	24,980
PEN/DMAc/PEG*6000*		10			72	30,643
PEN/DMAc/PEG*10000*			10		72	31,676

The morphology of the membranes was observed by a scanning electron microscopy (SEM, Hitachi S-4800). For the cross-sectional morphology test, it needs to be quenched in liquid nitrogen, and all samples need to be subjected to gold spray treatment before testing.

The equilibrium water content (EWC) and porosity of membranes are determined by the classical gravimetric method. The specific formula is as follows:

$$EWC(\%) = \frac{(W_w - W_d)}{W_w} \times 100\% \quad (1)$$

$$Porosity = \frac{(W_w - W_d)}{(\rho_w \times V)} \quad (2)$$

where, W_w and W_d are the weight of the membrane in wet and dry states (g), respectively; ρ_w is the density (g/cm^3) of pure water and V is the effective volume of the membrane in the wet state (cm^3).

The mean pore radius (r_m) for membrane surfaces was calculated using the Guerout-Elford-Ferry equation on the basis of the pure water flux, transmembrane pressure, and porosity parameters.

$$r_m = \sqrt{\frac{[(2.9 - 1.75\varepsilon) \times 8\eta l J_w]}{(\varepsilon \Delta P)}} \quad (3)$$

where, ε is the porosity of the membrane, η is the viscosity of water (8.9×10^{-4} Pa·s), l is the mean thickness of the membrane, J_w is the pure water flux, and ΔP is the operating pressure (0.1 mPa).

The residual of PEG in prepared PEN membranes was characterized by Fourier Transform Infrared spectroscopy (FTIR-ATR, Nicolet 8700) at a resolution of 4 cm^{-1} in the scanning range of 400–4,000 cm^{-1}, and differential scanning calorimetry (DSC250) at a heating rate of 10 °C/min in a nitrogen flow of 40 mL/min.

The water contact angle (WCA) of the membrane was measured using a dynamic contact angle meter (XG-CAMC3). A water droplet of 2 μL was dropped onto the membrane surface using a motorized controlled microsyringe. The image of the water droplet on the membrane surface was captured and the WCA value was measured by using imaging software. The WCA of each membrane was measured at lots of random points and the reported value is the average of these measurements.

Membrane performance evaluation

The permeation experiments were carried out in a cross-flow filter cell (FMT FlowMem-0002). Inside the cell, a rectangular membrane with an effective filtration area of 20 cm^2 was placed over a rubber washer support. The fresh membrane was firstly compacted with deionized water under 260 kPa for 4 h to obtain a stable pure water flux (PWF), then PWF was measured at a changing transmembrane pressure (ΔP ranging from 0–260 kPa). PWF, compaction factor (CF) and hydraulic permeability (P_m) were calculated, using the following equations:

$$J_w = \frac{Q}{(A \cdot \Delta T)} \tag{4}$$

$$CF = \frac{PWF_{\text{Initial}}}{PWF_{\text{Steadystate}}} \tag{5}$$

$$P_m = \frac{J_w}{\Delta p} \tag{6}$$

where, J_w is PWF ($L{\cdot}m^{-2}{\cdot}h^{-1}$), Q is volume of water permeated (L), A is effective filtration area (m^2) and ΔT is sampling time (h), CF is the ratio of initial pure water flux ($PWF_{Initial}$) to steady-state pure water flux ($PWF_{Steadystate}$), P_m is hydraulic permeability ($L{\cdot}m^{-2}{\cdot}h^{-1}{\cdot}kPa^{-1}$); ΔP is transmembrane pressure (kPa).

The rejection of membranes for contaminants was carried out by the membrane module (FMT FlowMem-0002), under a pressure of 100 kPa, using BSA solution (1,000 $mg{\cdot}L^{-1}$ of BSA in phosphate buffer solution (PBS), pH = 7.4) as a feed solution. The BSA concentration in permeate was determined using a UV-vis spectrophotometer (PerkinElmer Precisely, Lambda950) at a wavelength of 280 nm. The rejection ratio of BSA was determined as follows:

$$R(\%) = \left(1 - \frac{C_p}{C_f}\right) \times 100\% \tag{7}$$

where, C_p and C_f are the BSA concentrations in permeate and feed ($mg{\cdot}L^{-1}$), respectively.

Dynamic antifouling test

Under a pressure of 100 kPa, the antifouling test was performed as following. First, the pure water flux (F_{w1}) was measured for 45 min, followed by ultrafiltration of 1 g/L BSA solution (F_p) for the next 45 min. Then the membrane was removed from the filter and thoroughly cleaned with DI water. Finally, the pure water flux (F_{w2}) was measured again. The total fouling ratio (R_t) is composed of reversible fouling (R_r) and irreversible fouling (R_{ir}). The reversible fouling of membrane is caused by concentration polarization while the irreversible fouling is ascribed to the adsorption and deposition of proteins on the membrane surface. R_t, R_r, R_{ir}, and the flux recovery ratio (FRR) of the membrane after protein filtration were calculated using Equations (8)–(11), respectively:

$$R_t(\%) = \left(1 - \frac{F_p}{F_{w1}}\right) \times 100\% \tag{8}$$

$$R_r(\%) = \left[\frac{(F_{w2} - F_p)}{F_{w1}}\right] \times 100\% \tag{9}$$

$$R_{ir}(\%) = \left[\frac{(F_{w1} - F_{w2})}{F_{w1}}\right] \times 100\% \tag{10}$$

$$FRR(\%) = \frac{F_{w2}}{F_{w1}} \times 100\% \tag{11}$$

where, F_{w1} is the pure water flux, F_p is the permeate flux of the BSA solution, and F_{w2} is the pure water flux of the cleaned membrane ($L{\cdot}m^{-2}{\cdot}h^{-1}$).

RESULTS AND DISCUSSION

Apparent viscosity of the casting solution

It is well known that from the perspective of kinetic phase-separation, the apparent viscosity of the casting solution plays a critical effect in the forming of polymeric membrane. The influence of solvent as well as additive on the apparent viscosity of the casting solution was studied first. As listed in Table 1, the viscosity of the casting solution using NMP as solvent is about twice those using DMAc as solvent, which could be caused by poorer solubility of PEN in NMP compared with DMAc. In a concentrated polymer solution, the polymer chains tend to entangle with each other to increase their movement resistance at poor solubility, so the apparent viscosity of the solution increased. Additives also affect the casting solution viscosity significantly. In both solvent systems, the same trend of viscosity change can be observed with addition of different molecular weights of PEG. A low molecule additive, such as PEG*400*, reduced the viscosity of the casting solution, because it played a role in solvent dilution. Higher molecule additives, such as

PEG*6000* and PEG*10000*, can significantly increase the viscosity, and the viscosity change of the casting solution is positively correlated with the molecular weight.

Morphological study

Micromorphology of polymeric membranes was analyzed by scanning electron microscopy. Figure 2 shows the SEM image of the cross-section of membranes prepared by different solvents and additives. All of the membranes formed in the NMP system had a typical asymmetric membrane structure consisting of a dense top layer and porous finger-like structure sublayer. For the DMAc system, the membrane made by pure PEN solution with DMAc exhibited a complete sponge-like sublayer structure, the asymmetric structures begin to appear with the addition of PEG, and with the increasing of PEG molecular weight, the finger-like structure increased while the sponge-like pores decreased in the sublayer. Normally, the good compatibility of NMP and DMAc with water makes it easier for instantaneous demixing to form sublayer structures with finger-like pores when being used as solvents in the casting solution (Htrathmann & Kock 1997; Cheng *et al.* 2001). For the PEN/DMAc membrane, however, it showed a complete sponge-like sublayer structure. The long exposure time for membrane forming and the good solubility of PEN in DMAc could be the reason (Su *et al.* 2009). The nascent membrane absorbs a certain amount of water vapor before immersing in the coagulation bath, which causes the droplet size of the polymer-lean phase to be smaller and further coarsened. In both two systems, the increase of PEG molecular weight increases the thermodynamic instability degree of the casting solution, the exchange rate between solvent and non-solvent becomes faster, promoting the formation of macrovoids, and also improving the porosity and permeability of those membranes.

Figure 3 shows the SEM images of the top surfaces of the membranes. It is obvious that the surfaces of the pure PEN membranes prepared in two pure solvent systems are dense and nonporous. With the addition of PEG, the

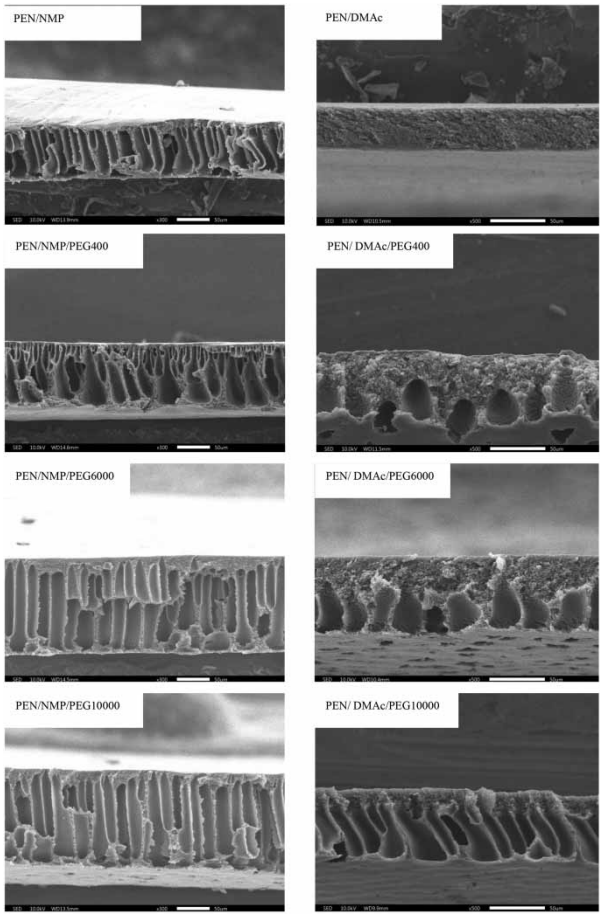

Figure 2 | SEM images of the membranes' cross-sections.

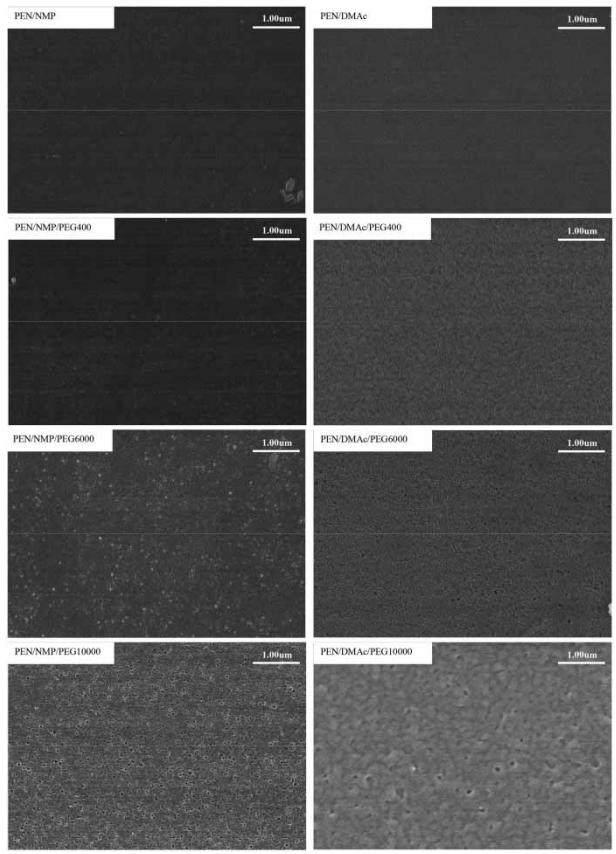

Figure 3 | SEM images of the membranes' top surface.

pores gradually appeared, and the pore size as well as the pore number increased with the increasing molecular weight of PEG. Meanwhile, a nodule/aggregate surface structure began to appear, and it became more apparent with the molecular weight of PEG increased, especially for DMAc system. As described by Boom *et al.* (Boom *et al.* 2011), the formation of such nodule surface morphology can be understood as the separation of the rich-phase polymer on the surface of the membrane by nucleation and growth, which also increases the connectivity between the pores. For a higher molecular weight PEG system, the lower mobility it is when immersed in the coagulation bath, resulting in a more obvious nodular on the membrane surface by the spinodal mixing.

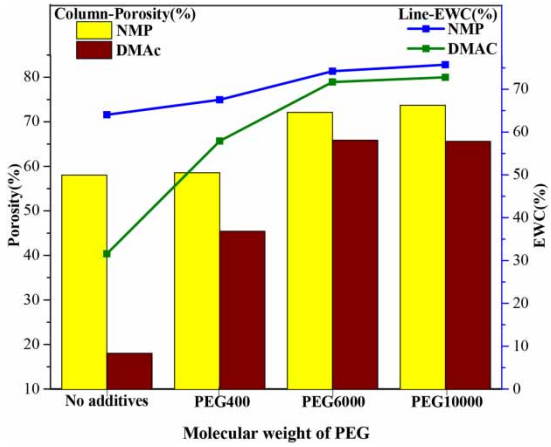

Figure 4 | Effect of PEG molecular weight on EWC and porosity.

Structural parameters of membranes

Table 2 listed the average values of EWC, porosity and r_m of each membrane calculated by Equations (1)–(3). The influence of solvent and PEG molecular weight on these two parameters of PEN membranes are also shown in Figure 4.

The porosity of PEN membranes prepared by NMP solvent system are larger than the DMAc system. For the PEN/NMP membrane, the porosity is 0.55, which is about triple that of the PEN/DMAc membrane. Since the porosity of the membrane is closely related to the EWC value, similar results also observed. The EWC value of PEN/NMP membrane is 64%, which is more than twice of that of PEN/DMAc membrane. This result is consistent with the Figure 2 cross-sectional SEM observation, and poorer solubility of the polymer in NMP could be the reason. For both solvent systems, the porosity and EWC values of membranes increased with the adding of PEG, and r_m of the membrane surface was positively correlated with the molecular weight of the added PEG. For PEN/DMAc/PEG*X* membranes, this influence is remarkable. With the adding of PEG*400*, the porosity increased from 0.18 to 0.45 and the EWC values increased from 31.6% to 57.9%, respectively. As molecular weight of PEG additive increases to 6,000, these values increased to 0.66 and 71.7%, respectively. Further increasing the molecular weight to 10,000 caused no significant increase for both values. Similar trend but with less values changing can be observed for the PEN/NMP/PEG*X* membranes. The variation of porosity can be explained based on the trade-off between the thermodynamic instability and kinetic rheological behavior of the casting solution (Zhao *et al.* 2011). On one hand, the addition of PEG destroyed the thermodynamic stability of the casting solution by reducing the miscibility of each component. On the other hand, it causes kinetic hindrance against phase separation by increasing the viscosity of the solution. Two competing effects jointly determine the final structure of the membrane. Therefore, the increase in the porosity of the film using PEG*6000* as additive may be due to its influence on the thermodynamic instability of the casting solution is dominant, which makes the prepared film more loose and of higher porosity (Chakrabarty *et al.* 2008).

Analysis for residual of PEG in prepared PEN membranes

DSC experiment was carried out to check the residual of PEG in the prepared PEN/NMP/PEG*X* membranes. For all of these PEN/NMP/PEG*X* membranes, only one tg with similar values can be observed (Figure 5), which

Table 2 | Values of some characterization parameters of PEN membranes

	PEN/NMP/PEG*X*				PEN/DMAc/PEG*X*			
Membranes	**No PEG**	**PEG *400***	**PEG *6000***	**PEG *10000***	**No PEG**	**PEG *400***	**PEG *6000***	**PEG *10000***
EWC (%)	64.0	67.6	74.2	75.7	31.6	57.9	71.7	72.8
Porosity	0.55	0.59	0.72	0.74	0.18	0.45	0.66	0.66
r_m(nm)	0	22.9	26.3	27.5	0	23.4	25.7	26.4

means that there is almost no residue of PEG in the PEN membrane matrix (Susantoa & Ulbricht 2009).

FTIR analysis was also used to check the residual of PEG in the membranes. All of the PEN/NMP/PEG*X* membranes have similar FTIR-ATR spectra, as shown in Figure 6. Two peaks at 2,970 and 2,863 cm^{-1}, which were associated to the C-H stretching of -CH_3 group, respectively, can be observed. The sharp absorption peak at 2,231 cm^{-1} is the characteristic absorption peak of -CN on the chain of poly (arylene ether nitrile). No characteristic absorption peak of PEG appeared on the infrared spectra of PEN membranes with PEG adding. This further confirmed that PEG is almost completely eluted from the PEN membrane matrix after washing.

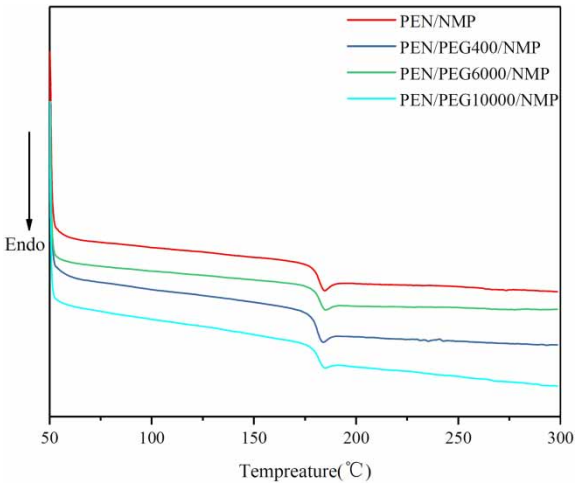

Figure 5 | DSC of PEN/NMP/PEG*X* membranes.

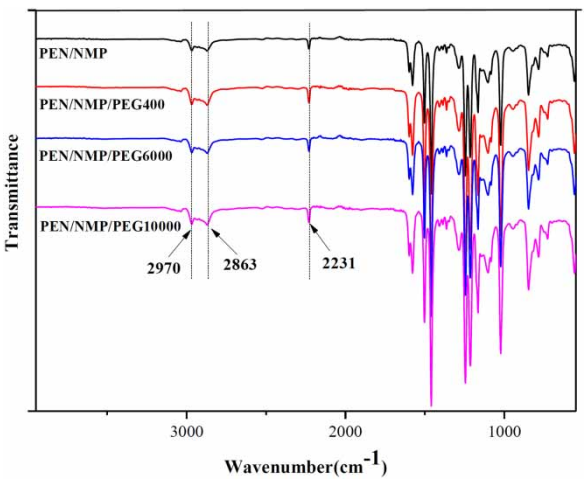

Figure 6 | FTIR-ATR spectra of fabricated PEN membranes.

Permeation experiments

The prepared PEN membranes are compacted at a constant transmembrane pressure of 260 kPa to obtain a stable flux. The PWF and CF of membranes are calculated using Equations (4) and (5). At least 5 sample tests were performed for each set of experimental data to ensure the authenticity of the data. It is worth mentioning that the missing data such as P_m and CF parameters for PEN/NMP and PEN/DMAc in Table 3 is because no water flux can be observed for these membranes even the driving pressure is as high as 0.26 MPa for compaction experiments. The PEN membranes without PEG additive is almost dense and non-porous, which can be confirmed by a high-magnification SEM image (Figure 3).

Figures 7 and 8 showed the effect of molecular weight of PEG on CF and P_m of membranes in a two solvent system, respectively. The PWF of all membranes gradually declined with time and reached a steady state within 1–2 h. The PWF of membranes with higher molecular weight additive dropped faster, but still kept a higher steady-state PWF. The average CF values for membranes are presented in Table 3. As the PEG molecular weight increases from 400 to 10,000, the CF increases from 1.08 to 1.35 for PEN/NMP/PEG*X* membranes, and from 1.15 to 1.62 for PEN/DMAc/PEG*X* membranes, respectively. PWF is more related to the size and number of pores on the membrane surface, while CF is determined by the macrovoids inside the membrane. The addition of PEG into the casting solution can promote the formation of macropores inside the membrane sublayer. Meanwhile, the increase of PEG

Table 3 | CF and P_m parameters of PEN membranes

	PEN/NMP/PEG*X*				PEN/DMAc/PEG*X*			
Membranes	**No additive**	**PEG *400***	**PEG *6000***	**PEG *10000***	**No additive**	**PEG *400***	**PEG *6000***	**PEG *10000***
CF	–	1.08	1.30	1.35	–	1.15	1.58	1.62
P_m ($L{\cdot}m^{-2}{\cdot}h^{-1}{\cdot}kPa^{-1}$)	–	0.50	0.94	1.13	–	0.67	0.89	0.95
WCA(°)	83.1 ± 1.4	79.3 ± 0.7	78.5 ± 2.0	78.8 ± 2.1	80.2 ± 1.6	76.3 ± 1.2	76.1 ± 1.3	75.3 ± 2.1

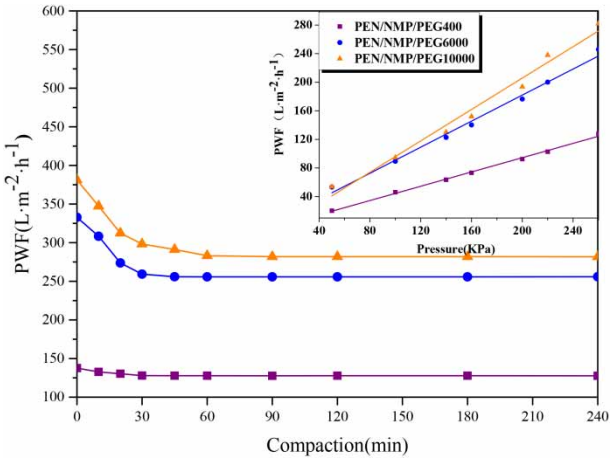

Figure 7 | Effect of molecular weight of PEG on CF and P_m in NMP system.

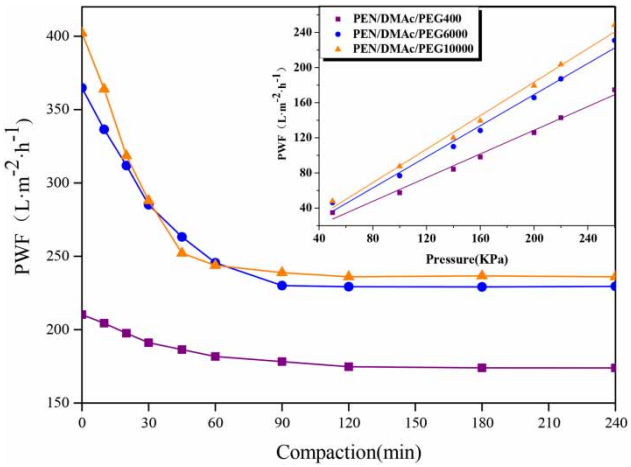

Figure 8 | Effect of molecular weight of PEG on CF and P_m in DMAc system.

molecular weight will lead to a more thermodynamically unstable casting solution and a faster phase separation, resulting in a higher porosity membrane. There are more macrovoids in the membrane sublayer, the larger CF of the membrane is, and the membrane is more easily compacted denser, resulting in the reducing the pore size as well as the flux. Compared with PEN/DMAc/PEG*X* membranes, PEN/NMP/PEG*X* membranes had higher porosity and more finger-like pores, but exhibited a lower CF, which may be mainly related to the finger-like structure in the sublayer. It can be clearly observed from the cross-sectional SEM that the finger-likes pores in the sublayer of PEN/NMP/PEG*X* membranes are closely arranged and interpenetrated to play a role of strength support; while the finger-like structures in the PEN/DMAc/PEG*X* membrane sublayer have poor penetration, but larger pore diameter. The closer to the bottom, the larger the pores and the easier it is to be compacted under pressure, leading to a significant increase in CF.

The changes in PWF under various transmembrane pressures of the compacted membranes are shown in Figures 7 and 8. A liner relationship between the PWF and transmembrane pressure can be observed for membranes within the pressure range of 0–260 kPa. For a particular pressure, an increasing of PWF with PEG molecular weight increasing can be found for both solvents. P_m determined by the slope of the linear fit of the discrete points using Equation (6), has been listed in Table 3. Obviously, the P_m of membrane increases as the additive molecular weight increases. When PEG molecular weight increases from 400 to 10,000, P_m values increases from 0.50 to 1.13 ($L \cdot m^{-2} \cdot h^{-1} \cdot kPa^{-1}$) and from 0.67 to 0.95 ($L \cdot m^{-2} \cdot h^{-1} \cdot kPa^{-1}$) for PEN/NMP/PEG*X* and PEN/DMAc/PEG*X*, respectively.

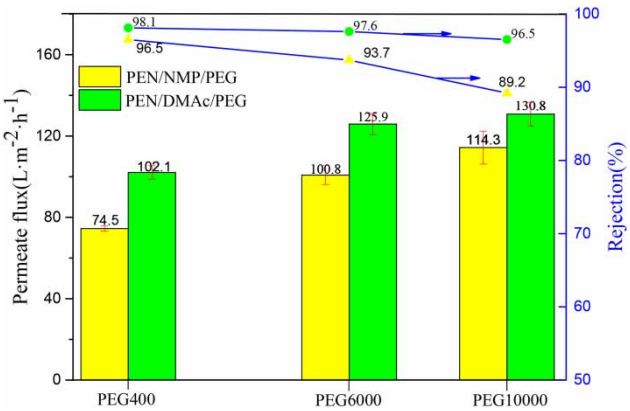

Figure 9 | Effect of molecular weight of PEG and solvent on permeate flux and rejection for PEN membranes.

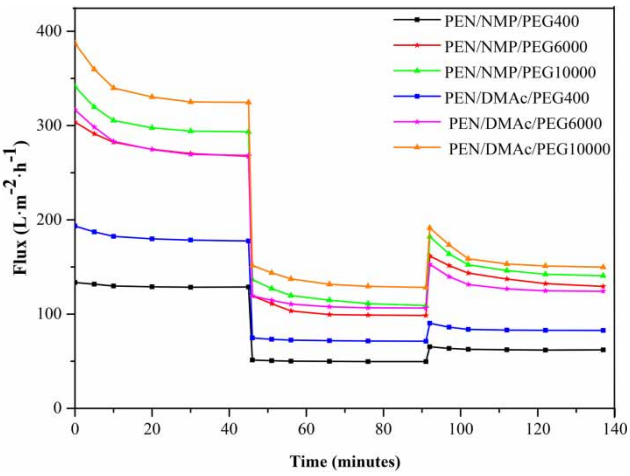

Figure 10 | Time-dependent fluctuation of PWF and BSA solution flux in one cycle.

Table 4 | Membrane antifouling performance parameters

	PEN/NMP/PEG*X*				PEN/DMAc/PEG*X*			
Membranes	**No additive**	**PEG *400***	**PEG 6000**	**PEG *10000***	**No additive**	**PEG *400***	**PEG *6000***	**PEG *10000***
FRR (%)	–	48.2	48.4	47.9	–	46.6	46.3	46.1
R_t (%)	–	61.5	63.1	62.8	–	59.9	60.4	60.5
R_r (%)	–	9.7	11.5	10.7	–	6.4	6.7	6.6
R_{ir} (%)	–	51.8	51.6	52.1	–	53.4	53.7	53.9

This result clearly revealed the significant influence of additive on the permeability of prepared membranes.

The selective permeability of membrane was evaluated by the rejection of BSA solution and the results are shown in Figure 9. For both types of membranes, the traditional trade-off between permeate flux and rejection ratio can be observed. When the molecular weight of additive increases, the permeate flux gradually increases, and the BSA rejection ratio decreases. The membranes prepared using DMAc as solvent has better performance compared with those by NMP, and their rejection ratios are all maintained at a level above 96.5%.

Antifouling performance test

The fouling experiments was carried out and the results are shown in Figure 10. As mentioned in 3.5 Permeation experiments, the dynamic antifouling performance of PEN/NMP and PEN/DMAc cannot be directly obtained due to the dense and non-porous membrane surface. For the remaining membranes, the decline in PWF was observed during the first filtration process, then a sharp decline of flux was observed when the BSA solution was used as feed, which could be caused by the deposition and adhesion of BSA on the membrane surface. After thoroughly washing with deionized water, the fluxes of all membranes cannot be completely recovered due to irreversible fouling. The specific antifouling property parameters have been listed in Table 4. Since PEG is eluted from the membrane surface during the membrane forming process, the choice of solvent and molecular weight of PEG only affects the antifouling performance of the membrane surface by forming different membrane structures during the phase inversion process. The hydrophilic additive PEG is not directly loaded in the membrane matrix to affect the hydrophilicity of the membrane surface. So, there is no significant difference in the related antifouling performance parameters of PEN/NMP/PEG*X* and PEN/DMAc/PEG*X*.

CONCLUSION

PEN flat sheet ultrafiltration membranes were prepared with casting solutions containing PEN/NMP/PEG*X* and PEN/DMAc/PEG*X*, respectively, via NIPS. Both the solvent and additive can significantly affect the structures and properties of the prepared membranes, especially the additive. PEG changes the rheological properties of the casting solution system. Low molecular weight PEG*400* behaves as a plasticizer and reduces viscosity of the casting solution, while higher molecular weight PEG*6000* and PEG*10000* obviously increase the viscosity. The addition of PEG effectively promotes the formation of macrovoids in the membranes. With the increase of PEG molecular weight, the thermodynamic instability of the casting solution dominates the phase separation process, which induces the formation of a more porous structure. The CF, EWC, Porosity and permeability of those membranes improved significantly with the increase of additive molecular weight. The PEN flat sheet ultrafiltration membranes prepared by using DMAc as solvent showed a higher permeate flux compared with those by NMP solvent (102.0 to 130.8 $L{\cdot}m^{-2}{\cdot}h^{-1}$ *vs.* 74.5 to 114.3 $L{\cdot}m^{-2}{\cdot}h^{-1}$ under a 100 kPa pressure-driven as PEG molecular weight increasing from 400 to 10,000 Da). PEN/DMAc/PEG*X* membranes also exhibit outstanding rejection property, and their R for BSA are all above 96.5%.

ACKNOWLEDGEMENTS

This work was supported by Research Startup program of Donghua University (285-07-005702).

DATA AVAILABILITY STATEMENT

All relevant data are included in the paper or its Supplementary Information.

REFERENCES

Boom, R. M., Rolevink, H. W. W., Boomgaard, T. V. D. & Smolders, C. A. 2011 Microscopic structures in phase inversion membranes: the use of polymer blends for membrane formation by immersion precipitation. *Macromol. Symp.* **69** (1), 133–140.

Braeken, L., Bettens, B., Boussu, K., Meeren, P. V. D., Cocquyt, J. & Vermant, J. 2006 Transport mechanisms of dissolved organic compounds in aqueous solution during nanofiltration. *J. Membr. Sci.* **279** (1–2), 311–319.

Chakrabarty, B., Ghoshal, A. K. & Purkait, M. K. 2008 Effect of molecular weight of peg on membrane morphology and transport properties. *J. Membr. Sci.* **309** (1–2), 209–221.

Cheng, L. P., Young, T. J. & Chuang, W. Y. 2001 The formation mechanism of membranes prepared from the nonsolvent-solvent-crystalline polymer system. *Polymer.* **42** (2), 443–451.

Gao, Z. F., Shi, G. M. & Cui, Y. 2018 Organic solvent nanofiltration (OSN) membranes made from plasma grafting of polyethylene glycol on cross-linked polyimide ultrafiltration substrates. *J. Membr. Sci.* **565** (1), 169–178.

Gutmann, B. & Obermayer, D. 2010 Sintered silicon carbide: a new ceramic vessel material for microwave chemistry in single-mode reactors. *Chem. Eur. J.* **16** (40), 12182–12194.

Han, M. J. & Nam, S. T. 2002 Thermodynamic and rheological variation in polysulfone solution by PVP and its effect in the preparation of phase inversion membrane. *J. Membr. Sci.* **202** (1–2), 55–61.

Htrathmann, H. & Kock, K. 1997 The formation mechanism of phase inversion membranes. *Desalination* **21** (3), 241–249.

Idris, A., Zain, N. M. & Noordin, M. Y. 2007 Synthesis, characterization and performance of asymmetric polyethersulfone (PES) ultrafiltration membranes with polyethylene glycol of different molecular weights as additives. *Desalination* **207** (1–3), 324–339.

Koehler, J. A., Ulbricht, M. & Belfort, G. 1997 Intermolecular forces between proteins and polymer films with relevance to filtration. *Langmuir.* **13** (15), 4162–4171.

Lignier, P., Estager, J., Kardos, N., Gravouil, L. & Draye, M. 2011 Swift and efficient sono-hydrolysis of nitriles to carboxylic acids under basic condition: role of the oxide anion radical in the hydrolysis mechanism. *Ultrason. Sonochem.* **18** (1), 28–31.

Machado, P. S. T. & Habert, A. C. 1999 Membrane formation mechanism based on precipitation kinetics and membrane morphology: flat and hollow fiber polysulfone membranes. *J. Membr. Sci.* **155** (2), 171–183.

Madaeni, S. S. & Rahimpour, A. 2010 Effect of type of solvent and non-solvents on morphology and performance of polysulfone and polyethersulfone ultrafiltration membranes for milk concentration. *Polym. Adv. Technol.* **16** (10), 717–724.

Matsuo, S., Murakami, T. & Takasawa, R. 1993 Synthesis and properties of new crystalline poly (arylene ether nitriles). *J. Polym. Sci. Part A: Polym Chem.* **31** (13), 3439–3446.

Miteva, M., Christova, D., Ivanova, S. & Petrov, S. 2017 Effect of hydrophobically modified pva on the temperature-responsive structure and permeation of pan-based composite ultrafiltration membranes. *Polym. Bull.* **75** (7), 2805–2817.

Oskoui, S. A., Vatanpour, V. & Khataee, A. 2019 Effect of different additives on the physicochemical properties and performance of NLDH/PVDF nanocomposite membrane. *Sep. Purif. Technol.* **209**, 921–935.

Park, J. Y., Acar, M. H., Akthakul, A., Kuhlman, W. & Mayes, A. M. 2006 Polysulfone-graft-poly (ethylene glycol) graft copolymers for surface modification of polysulfone membranes. *Biomaterials.* **27** (6), 856–865.

Pu, Z. & Lan, C. 2013 Influence of composition on the proton conductivity and mechanical properties of sulfonated poly (aryl ether nitrile) copolymers for proton exchange membranes. *J. Polym. Res.* **20** (11), 1–9.

Su, Y. S., Kuo, C. Y., Wang, D. M., Lai, J. Y., Deratani, A. & Pochat, C. 2009 Interplay of mass transfer, phase separation, and membrane morphology in vapor-induced phase separation. *J. Membr. Sci.* **338** (1–2), 17–28.

Sun, H. G. & Yang, X. B. 2018 Segregation-induced in situ hydrophilic modification of poly (vinylidene fluoride) ultrafiltration membranes via sticky poly (ethylene glycol) blending. *J. Membr. Sci.* **563**, 22–30.

Sun, W., Li, L., Chen, C. & Li, J. 2010 Effects of operation conditions, solvent and gelation bath on morphology and performance of ppesk asymmetric ultrafiltration membrane. *J. Appl. Polym. Sci.* **108** (6), 3662–3669.

Susantoa, H. & Ulbricht, M. 2009 Characteristics, performance and stability of polyethersulfone ultrafiltration membranes prepared by phase separation method using different macromolecular additives. *J. Membr. Sci.* **327** (1–2), 125–135.

Tang, H., Yang, J., Zhong, J., Zhao, R. & Liu, X. 2011 Synthesis and dielectric properties of polyarylene ether nitriles with high thermal stability and high mechanical strength. *Mater. Lett.* **65** (17), 2758–2761.

Weatherley, L. R. 1994 *Engineering Processes for Bioseparations*. Eng. Proc. Biosep., Butterworth-Heinemann, Oxford, UK. pp. 285–296.

Yi, Z., Zhu, L., Cheng, L., Zhu, B. K. & Xu, Y. Y. 2012 A readily modified polyethersulfone with amino-substituted groups: its amphiphilic copolymer synthesis and membrane application. *Polymer.* **53** (2), 350–358.

Zhang, W. L., Wang, Z. J. & Liu, X. B. 2019 A novel poly(arylene ether nitrile) ultrafiltration membrane for water purification and its antifouling property with in situ-generated SiO2 nanoparticles. *High. Perf. Polym.* **31** (8), 977–985.

Zhang, G. Y., Zhan, Y. Q. & He, S. J. 2020 Construction of superhydrophilic/underwater superoleophobic polydopamine-modified h-BN/poly(arylene ether nitrile) composite membrane for stable oil-water emulsions separation. *Polym. Adv. Technol.* **31** (5), 1007–1018.

Zhao, S., Wang, Z., Wei, X., Tian, X., Wang, J. & Yang, S. 2011 Comparision study of the effect of pvp and pani nanofibers additives on membrane formation mechanism, structure and performance. *J. Membr. Sci.* **385** (1–2), 110–122.

First received 31 July 2020; accepted in revised form 23 October 2020. Available online 5 November 2020